JOURNAL OF MATERIALS SCIENCE 29 (1994) 2071–2077

Surface modification of superdrawn polyoxymethylene fibres

Part II *Pull-out behaviour of the fibre–RFL adhesive–rubber system*

TAMIKUNI KOMATSU
Analytical Research Centre of Asahi Chemical Industry Co. Ltd, 2-1 Samijima, Fuji, Sizuoka 416, Japan

The pull-out fracture of surface-modified superdrawn polyoxymethylene fibres embedded in rubber is discussed from a fractographical viewpoint. The morphologies of the pull-out fracture plane were very similar to those of the fracture surface in single lap-joint tests and the true pull-out stress coincided with the shear strength of a single lap-joint, indicating that the pull-out failure is strongly related to single lap-joint shear fracture.

1. Introduction

Fibres of high modulus and strength such as carbon fibre, glass fibre, aramid yarn and ultradrawn fibre are widely used for various fibre-reinforced matrix composites. Adhesion of fibres to the matrix can be experimentally assessed by several fracture tests such as the pull-out [1–10] and micro-indentation [11] tests according to the usage of composites, and the fracture stress is usually found to depend on several parameters such as interfacial affinity, embedding length, fibre diameter and mechanical properties of the matrix [1–4, 10, 12, 13].

The fractography and fracture processes of composites have been energetically studied to clarify the characteristics of the interfacial adhesion between fibre and matrix. For example, a multi-stage fracture process including debonding and frictional slip was observed in the single-fibre pull-out behaviours of highly drawn polyethylene fibre, carbon fibre, and glass fibre embedded in epoxy matrices, and explained by double lap-joint theory [4], a modified fracture mechanics [6, 7], and a modified shear lag model [8, 9], respectively. In the case of cord–rubber composites, many efforts have been made in the surface treatment of cords to enhance interfacial adhesion but little on the study of the fracture mechanism [1, 3].

In the Part I, [14], surface modification of superdrawn polyoxymethylene fibres was applied to the fibre–RFL adhesive–rubber system, and such a high interfacial miscibility as causes cohesive failure of the fibre was attained. In this paper, the pull-out fracture process is discussed in terms of the morphology of the fracture surface.

2. Experimental procedure

2.1. Preparation of superdrawn polyoxymethylene fibres

Undrawn polyoxymethylene (POM) tubes with three different diameters, having outer diameters of 2.3, 3.2 and 4.5 mm and inner diameters of 0.8, 1.0 and 1.5 mm, respectively, were first prepared by extrusion of an acetal homopolymer (Asahi Chemical Industry Co., Tenac 3010). The undrawn POM tubes were continuously two-step drawn up to a draw ratio of 20 in compressed silicone oil and fibres with diameters of 0.50, 0.80 and 1.00 mm were obtained. The resulting fibres were completely washed with Freon 113 to remove silicone oil adhering to the fibre. Tensile strength and Young's modulus along the fibre axis were 1.8 and 40 GPa, respectively. The details were described in previous work [15, 16].

2.2. Preparation of surface-modified POM fibres

POM fibres were sand-blasted, surface-activated and dipped in RFL. Four activating agents with the following compositions (by weight) were used: (i) a 40% aqueous solution of resorcinol; (ii) a mixture of resorcinol (40 parts) and RF solution (60 parts); (iii) a mixture of resorcinol (40 parts), RFL solution (20 parts) and water (40 parts); (iv) a mixture of resorcinol (40 parts), RF solution (20 parts), RFL solution (20 parts) and water (20 parts). The preparations of modified fibres, RF and RFL solutions were carried out in the same way as described in Part I [14].

2.3. Measurement of pull-out strength

The resulting POM fibres were moulded with a compounded crude rubber used for automotive tyre carcasses into composite bars and followed by the T pull-out test (JIS L 1017(1983)), in the same way as described in the Part I [14]. Fluctuation in the observed pull-out load was within about $\pm 4\%$. The pull-out stress of the fibre in the rubber matrix was

0022–2461

calculated from the equation

$$T = F/\pi DL \quad (1)$$

where T is the pull-out tensile stress, F the observed pull-out load, D the fibre diameter and L the adhesive length. The diameter D was taken as the diameter of the intact fibre, since the weight of fibres hardly changed before and after the treatments. For comparison, RFL-dipped nylon 66 cord (Asahi Chemical Industry Co., Leona 66, 1260/1/2 cords), aramid cord treated with epoxy–RFL adhesives (Toray–du Pont Co., Kevlar T–49, 1500/1/2 cords) and aramid cord coated with epoxy–RFL adhesives (Teijin Co., Technora, 1500/2/3 cords), were assessed in the same way as above. The cord diameter (in centimetres) was also calculated from the cord denier d from the relationship [1].

$$D = \left(\frac{4d}{9 \times 10^5 \pi \rho \times 0.77}\right)^{0.5}$$

where ρ is the specific gravity of polymer; those of nyron 66, Kevlar and Technora cords were put at 1.14, 1.44 and 1.39, respectively.

2.4. Measurement of shear strength by single lap-joint test

The shear strength of the POM fibres was measured by a tensile test using a single lap-joint specimen as shown in Fig. 1. The specimen was prepared by cutting the fibre carefully along the fibre centre-line with a cutter knife. Measurement was carried out five times according to the following conditions: sample length, 200 mm; lap length, 5, 10, 15 and 20 mm; crosshead speed, 100 mm min^{-1}. The shear strength σ was calculated from

$$\sigma = F/DL \quad (2)$$

where F is the fracture load, D the fibre diameter and L the lap length. Fluctuation in the strength obtained was about $\pm$ 5%.

2.5. Surface observation

The morphologies of the embedded region after pull-out and the fracture surface after the single lap-joint test were investigated by optical microscopy and scanning electron microscopy (SEM) (Hitachi S-430). The samples for SEM were lightly coated with gold by a vacuum coating unit. SEM observation was carried out at 5 kV.

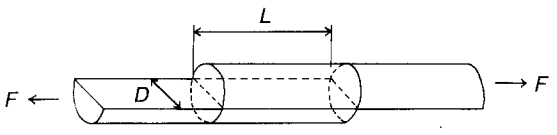

Figure 1 Specimen geometry for a single lap-joint test: F = pull-out load, D = the fibre diameter, L = lap length.

3. Results

3.1. Characteristics of the pull-out behaviour

The pull-out strength of the modified POM fibre–rubber system is given in Table I. The strength was in the sample order A > B > C ≃ D, although the difference is small. The morphological characteristics of the embedded region after the pull-out test were examined. Figs 2–5 show optical micrographs of the pull-out region of samples A to D. Sample A was almost entirely covered with rubber on one side of the surface and showed cohesive failure in some places and locally bonded rubber on the other side (Fig. 2). Sample B showed cohesive failure in many regions and bonding to rubber in some places (Fig. 3). Samples C and D were similar to sample B in the appearance on one side of the surface, but showed greater fractures across the fibrils on the other side, in which three types of failure morphology were found (Figs 4 and 5). These are (a) a slanting fracture of the POM fibre and adhesion of a fan-shaped rubber block, (b) a slanting fracture of the POM fibre and adhesion of a rubber coat, and (c) a slanting fracture over the whole embedded region on one side of the surface.

TABLE I Pull-out strength of modified POM fibres embedded in rubber: the fibre diameter was 0.8 mm and the adhesive length 10 mm

Sample	Pull-out load (N)	Pull-out strength (MPa)	Appearances of pull-out regions
A	310.7	12.4	Cohesive failure
B	346.9	13.8	Cohesive failure
C	364.6	14.5	Slanting fracture
D	365.5	14.6	Slanting fracture

Figure 2 Optical micrograph of the pull-out region of sample A, modified with resorcinol.

Figure 3 Optical micrograph of the pull-out region of sample B, modified with resorcinol including RF.

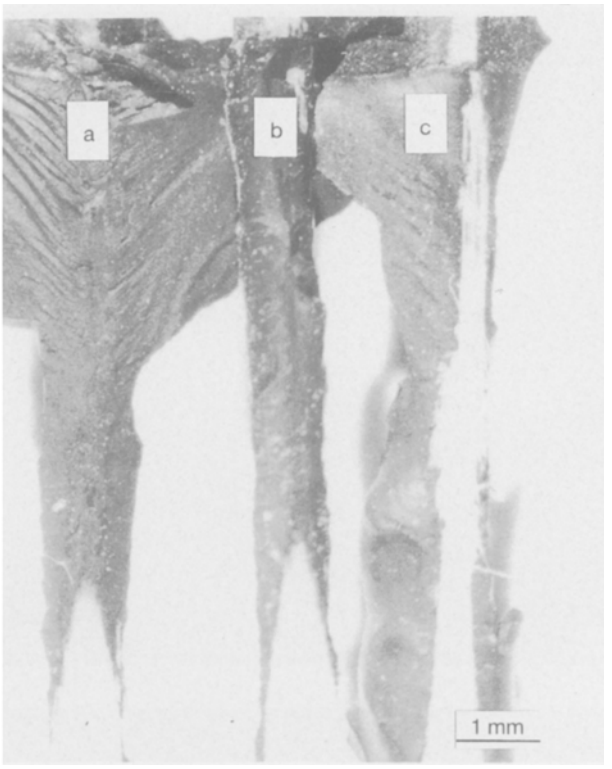

Figure 5 Optical micrograph of the pull-out region of sample D, modified with resorcinol including RF and RFL: (a) a slanting fracture of the fibre and adhesion of a fan-shaped rubber block, (b) a slanting fracture of the fibre and adhesion of a rubber coat, (c) a slanting fracture over the whole embedded region on one side of the fibre.

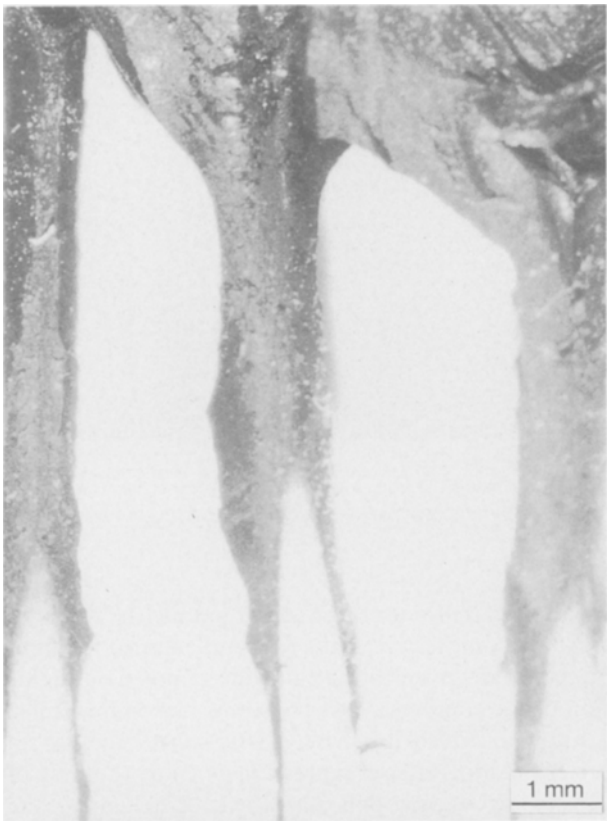

Figure 4 Optical micrograph of the pull-out region of sample C, modified with resorcinol including RFL.

In all types, many stress-lines exhibiting pulled-out traces were found on the surface of rubber adhering to the fibre, and a slanting fracture plane across the fibre cross-section was observed in the fracture surface of the fibre. Such a slanting fibre fracture is similar to the fracture mode of an oriented poly(ethylene terephthalate) sheet which fractures along the shear deformation band when tensile stress is applied slantingly to the orientation axis [17].

These appearances show two important results: (i) the pull-out process produces a shear fracture of the fibre; (ii) pull-out fracture is initiated by the initial debonding which causes a cohesive fracture of the fibre skin, and is rapidly transmitted across the internal fibrils. The cause of asymmetric fracture of the pulled-out specimen is not clear at present.

3.2. Fractography of the pull-out region

The morphology of the failure surface changed with the embedded position as found in Fig. 5. The morphology of the fracture surface generally includes information on the fracture process, so fractography of the fracture surface was investigated in detail by SEM.

Fig. 6 shows SEM micrographs of the slanting fracture surface of Fig. 5c and reveals the following: at the emergent fibre end a rough, fibrillated structure along the fibrils is found (Fig. 6a); at 4 mm down, vigorous tearing of fibrils (Fig. 6b); at 6 mm down, a comparatively smooth fracture plane (Fig. 6c); at the embedded end, a fairly smooth plane (Fig. 6d). This indicates that the pull-out failure proceeds in two stages: in the initial stage, stress concentration and tear-off failure occur in the fibre interface at the

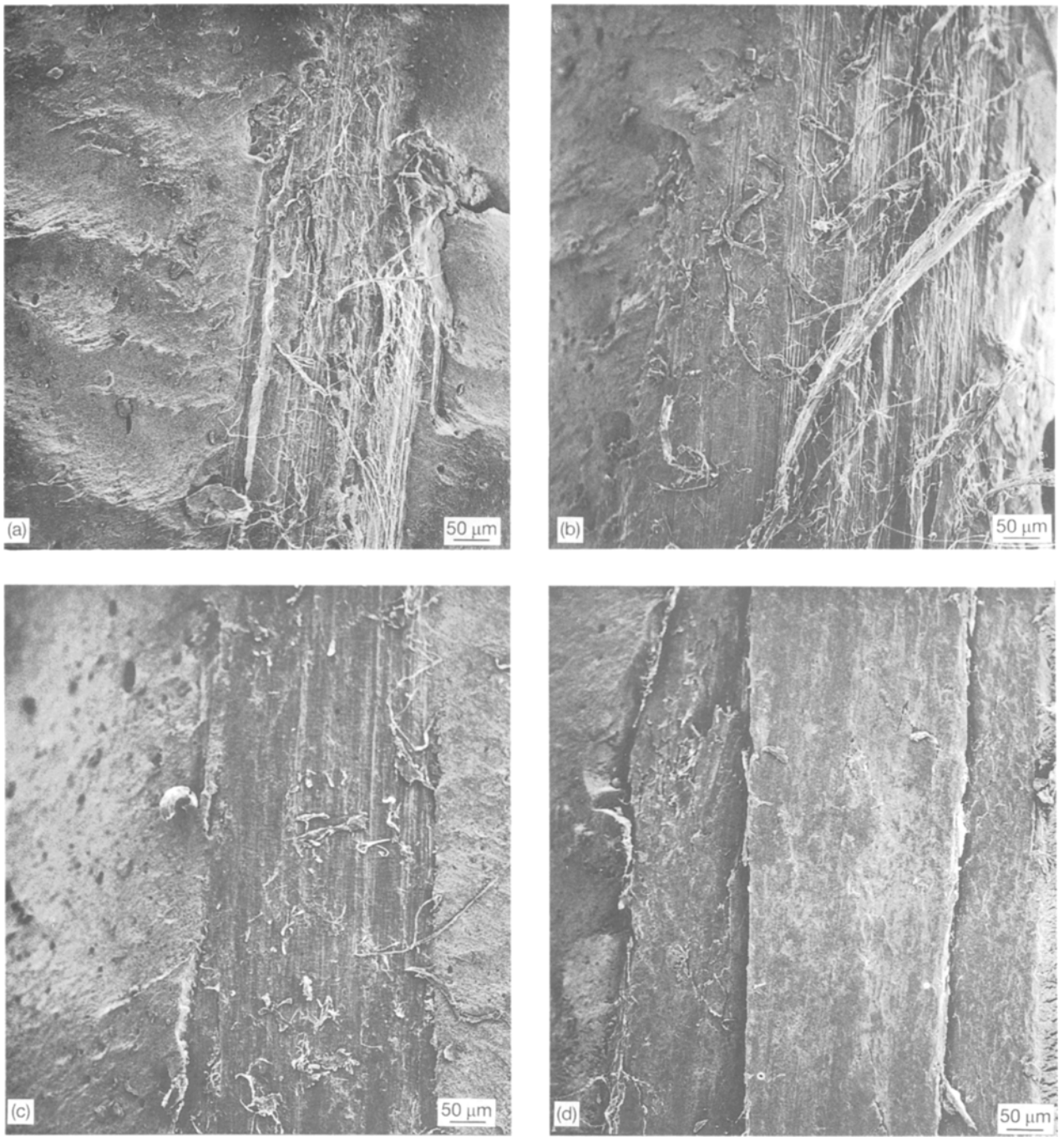

Figure 6 SEM micrographs of the fracture plane of pull-out sample D: (a) rough surface at the fibre emergent end, (b) tear fracture surface at 4 mm down from the emergent end, (c) smooth fracture surface at 6 mm down from the emergent end, (d) fairly smooth fracture surface at the embedded end.

emergent end and grow to a maximum at the position 4 mm down; in the second stage, fracture propagates rapidly into the fibre inside across fibrils towards the embedded end. The pull-out failure clearly shows a shear fracture plane, so fractography of a single lap-joint fracture surface was also investigated for comparison, as shown in Fig. 7. It can be seen that both fracture morphologies are very similar, suggesting a similarity between the two failure processes.

4. Discussion

4.1. Shear stress on the fracture plane

Fig. 8 illustrates a schematic representation of the pull-out fracture. In this model, it is hypothesized that an applied pull-out tensile stress parallel to the fibre axis and compressive stress perpendicular to the fibre direction are given to the embedded fibre. Consideration of the compressive stress seems reasonable, since a fibre embedded in a viscoelastic rubber matrix receives the transverse compression given by thinning of the matrix during pull-out. Shear stress along the slanting fracture plane, i.e. true pull-out strength τ(true), can be calculated on the basis of the surface area of the shear fracture plane, according to the equation

$$\tau(\text{true}) = 4F\sin\theta/\pi D^2 \quad (3)$$

where F is the pull-out load, θ the angle between the fracture plane and fibre axis and D the fibre diameter.

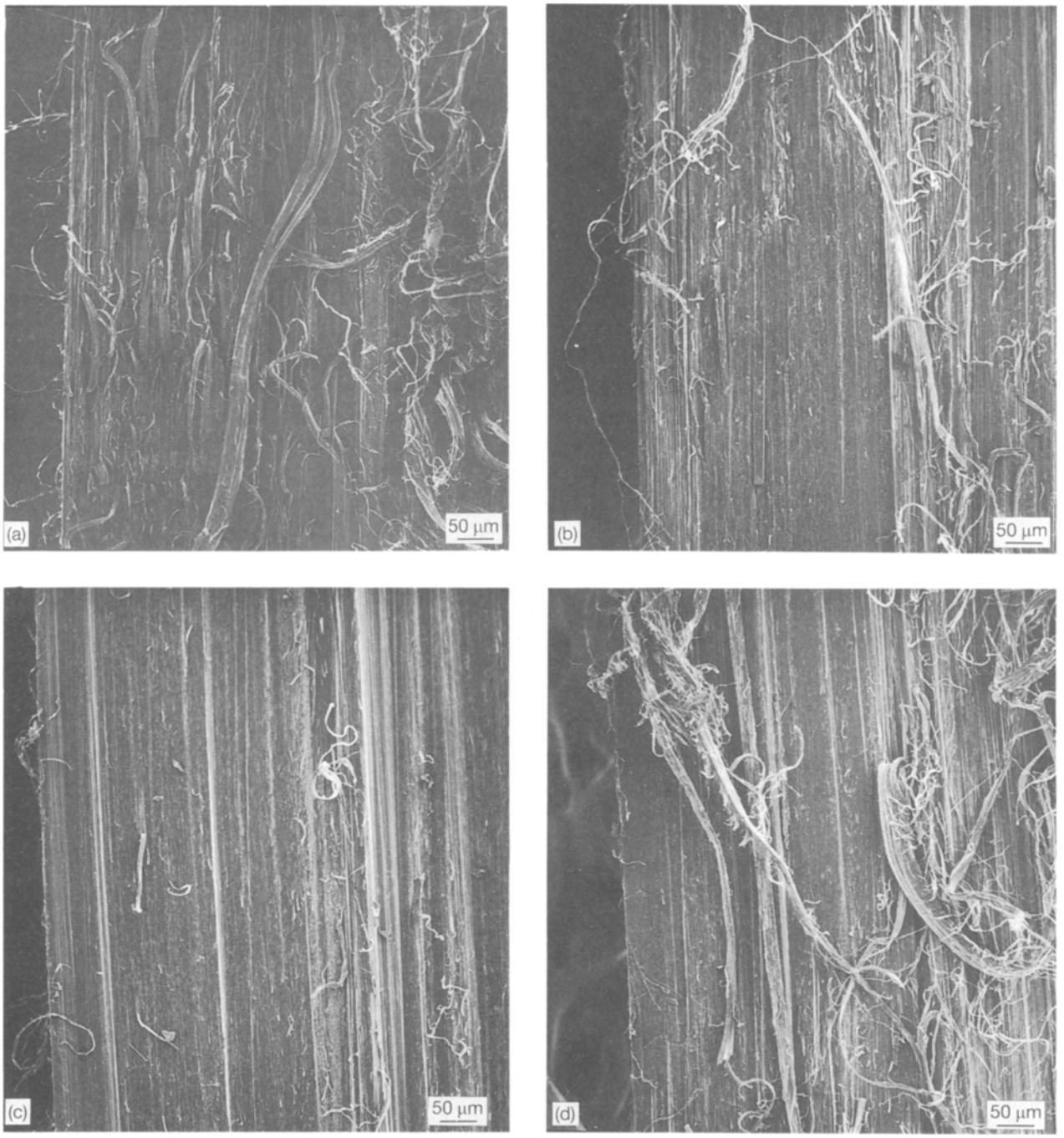

Figure 7 SEM micrographs of the fracture plane after the single lap-joint test: (a) the lap tip, (b) 4 mm down from the tip, (c) 6 mm down from the tip, (d) the lap end.

In the case of sample D, F was 365.5 N, θ was ca. 2.3° and D was 0.8 mm, thus τ(true) = 29.8 MPa. On the other hand, the measured single-lap shear strength of the same sample D was 30.4 MPa at a lap length of 10 mm, as shown in Fig. 9. The observed true pull-out stress coincides fairly well with the shear strength. This coincidence does not mean that the pull-out process can be perfectly explained by a single lap-joint model, since a single lap-joint test includes the complex mechanical problem that bending deformation occurs in addition to tensile deformation.

The problem has been already discussed of the stress concentration which remarkably increases with an increase in the lap length [18, 19] and the unbalanced stress distribution in which the shear strain at both edges of the lap length is much larger than the minimum strain at the centre [20]. The bending deformation in a single lap-joint can be successfully avoided in the double lap-joint system. For example, the pull-out adhesion of plasma-treated high-modulus polyethylene fibres to an epoxy resin has been discussed in terms of double lap-joint theory, in which the remarkable dependence of the stress on the adhesive length has been well explained [12]. However, the theory does not seem to fit the present composite system, since the pull-out strength hardly depends on the fibre diameter as will be discussed later.

4.2. Pull-out behaviour

Models of the single-fibre pull-out process have been recently presented on the basis of the pull-out behaviour

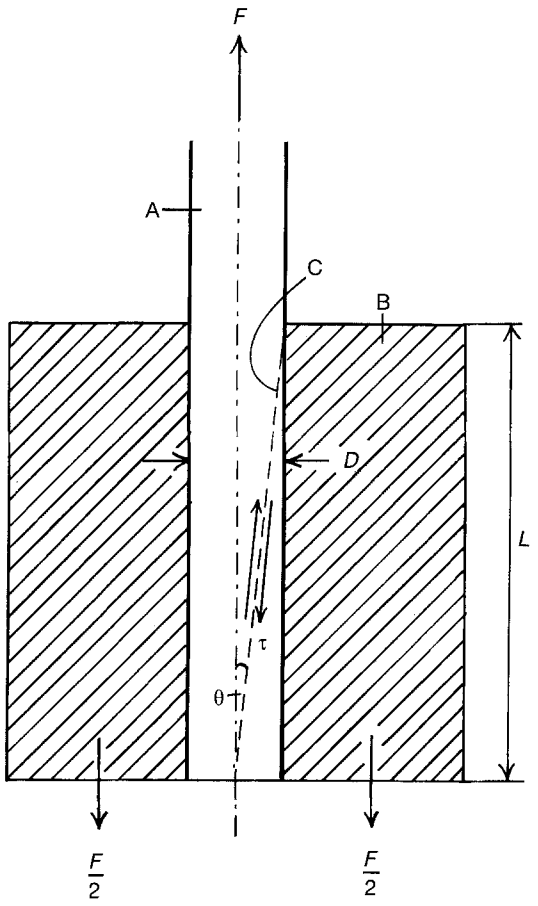

Figure 8 Schematic representation of a pull-out fracture of a surface-modified POM fibre embedded in the rubber matrix: (A) POM fibre, (B) rubber matrix, (C) fracture plane, D = fibre diameter, L = adhesive length, F = pull-out load, τ = shear stress along the fracture plane, θ = shear angle.

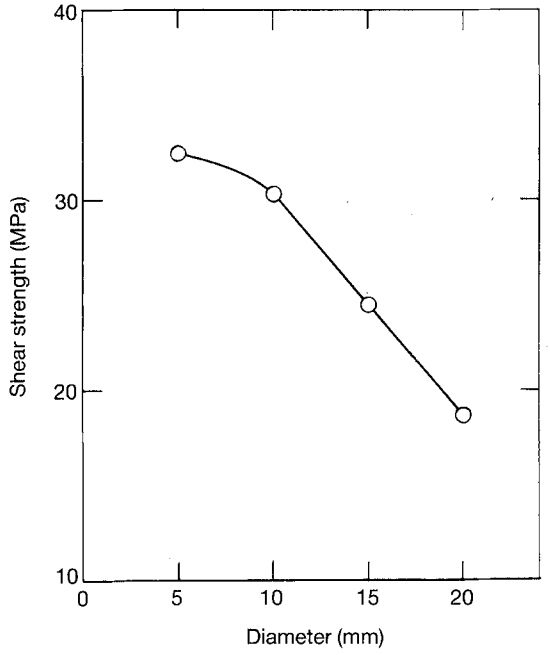

Figure 9 Shear strength of superdrawn POM fibres by the single lap-joint test, carried out for fibres with 0.8 mm diameter, a draw ratio of 20 and different lap lengths.

of carbon fibre embedded in an epoxy resin [6, 7], glass fibre embedded in a PP resin [8, 9], and glass fibre embedded in an epoxy resin and an HDPE resin [10], in which the experimental pull-out curves showed three failure processes: debonding crack initiation, a stick–slip process and a slip stage.

Pull-out curves like these were certainly observed in several composite systems consisting of superdrawn POM fibre only enhanced in specific surface area and a matrix (tyre rubber, urethane rubber, epoxy resin and unsaturated polyester resin). However, pull-out tests of the surface-modified POM fibre–rubber system showed a simple stress–strain curve like the single lap-joint test, indicating that the process is conducted by the initial debonding and includes no slippage. Although the mechanisms of pull-out and single-lap shear fracture are not sufficiently clear at present, the measurement of shear strength will be useful for estimating the pull-out adhesion.

4.3. Dependence of adhesion on fibre diameter

Fig. 10 shows a comparison of the pull-out load among the present POM fibre, nylon 66 and two aramid tyre cords. The pull-out loads for nylon and aramid cords lay in a straight line passing through the origin. As the slope of the line is the pull-out strength, this result means that the pull-out strength for these cords is independent of the cord diameter. The loads for the POM fibres also lay in a straight line passing through the origin, but the slope was larger than that for the cords. The pull-out strength obtained for the

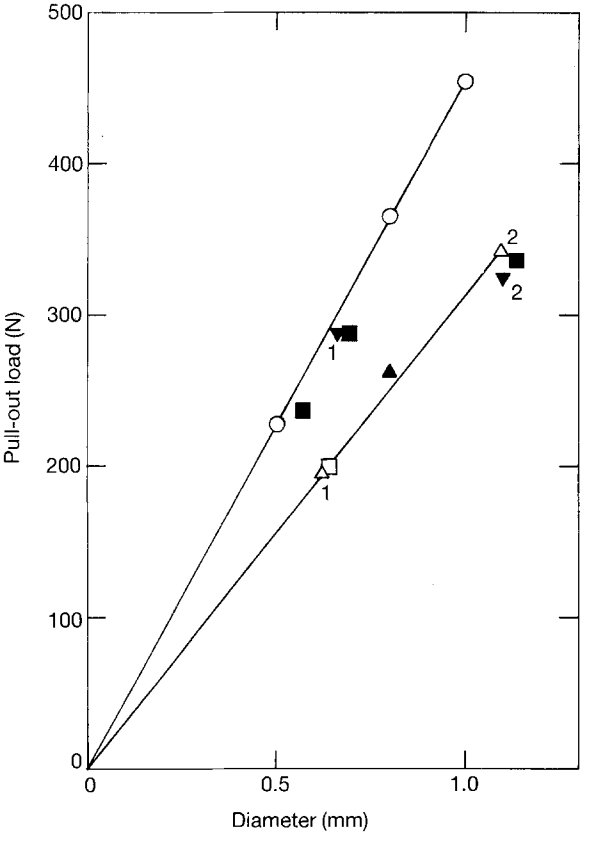

Figure 10 Relationship between fibre diameter and the pull-out load: (○) surface-modified POM fibres, (□) Leona 66 cord, (△1) Kevlar T-49 cord, (△2) Technora cord, (■) nylon 6 cords by Iyengar [1], (▲) Kevlar cord by Iyengar [2], (▼1) steel cord by Iyengar [2], (▼2) steel cord by Gent *et al.* [3].

POM fibres and the tyre cords was 14.6 and 10.1 MPa, respectively.

In addition, the reported strength for tyre cords is 13.4–8.4 MPa [1] for nylon cords, 10.4 MPa [2] for Kevlar cords, and 13.9 MPa [2] and 9.4 MPa [3] for brass-plated steel cords, as plotted on the same figure. In these cords, the nylon and steel cords decrease in strength on increasing the cord deniers differently from the Kevlar cords; this has been deduced to arise from the increased stress concentrations due to high pulling force [1] and Griffith's fracture process [3]. The POM fibres showed the highest strength in spite of the large diameter of the monofilament. This behaviour confirms the idea that the adhesion of the modified POM layer to an RFL layer is based on perfect interfacial miscibility, i.e. the present surface modification gives the highest affinity attainable in the fibre–RFL adhesive–rubber system.

5. Conclusions

The pull-out process of surface-modified superdrawn polyoxymethylene fibres embedded in rubber was discussed in terms of the morphology of the fracture plane. The pull-out failure is essentially a shear fracture which occurs in two stages: stress concentration occurs at the fibre emergent end and causes a tear failure, rapidly leading to a shear fracture across the fibrils. The morphologies of the pull-out failure plane were very similar to those of the shear fracture surface in a single lap-joint test. The true pull-out stress based on the surface area of the shear fracture plane coincided with the shear fracture strength of a single lap-joint. These results indicate that the pull-out failure strongly relates to a single lap-joint shear fracture. The pull-out adhesion is characterized by the linear dependence of the pull-out load on fibre diameter. This behaviour means that the proposed surface modification provides the ideal composite in the POM fibre–RFL adhesive–rubber matrix system.

References

1. Y. IYENGAR, *J. Appl. Polym. Sci.* **13** (1969) 353.
2. *Idem, ibid.* **22** (1978) 801.
3. A. N. GENT, G. S. F. RUSSELL, D. I. LIVINGSTON and D. W. NICHOLSON, *J. Mater. Sci.* **16** (1981) 949.
4. N. H. LADIZESKY and I. M. WARD, *ibid.* **18** (1983) 533.
5. L. S. SCHADLER, C. LAIRD, N. MELANITIS, C. GALIOTIS and J. C. F IGUEROA, *ibid.* **27** (1992) 1663.
6. J. K. KIM, C. BAILLIE and Y. W. MAI, *ibid.* **27** (1991) 3143.
7. L. M. CHOU, J. K. KIM and Y. W. MAI, *ibid.* **27** (1992) 3155
8. C. Y. YUE and W. L. CHEUNG, *ibid.* **27** (1992) 3173.
9. *Idem, ibid.* **27** (1992) 3181.
10. C. K. MOON, J. O. LEE, H. H. CHO and K. S. KIM, *J. Appl. Polym. Sci.* **45** (1992) 443.
11. S. W. WANG, A. KHAN and R. SANDS, *J. Mater. Sci. Lett.* **11** (1992) 739.
12. N. H. LADIZESKY and I. M. WARD, *J. Mater. Sci.* **24** (1989) 3763.
13. Y. L. HSIEH, G. BARRALL and S. XU, *Polymer* **33** (1992) 2143.
14. T. KOMATSU, *J. Mater. Sci.* **28** (1993) 000.
15. T. KOMATSU, S. ENOKI and A. AOSHIMA, *Polymer* **32** (1991) 1983.
16. *Idem, ibid.* **32** (1991) 1988.
17. I. M. WARD, *Polym. Eng. Sci.* **24** (1984) 724.
18. O. VOLKERSEN, *Luftfahrforshung* **15** (1/2) (1939) 41.
19. F. SZEPE, *Exp. Mech.* **6** (1966) 282.
20. N. H. LADIZESKY and I. M. WARD, *J. Mater. Sci.* **23** (1988) 72.

Received 26 August 1992
and accepted 3 February 1993